Supplementary Information

Iron-Induced Phase Engineering for High Color-Purity Blue LEDs in Perovskites

Youngchae Cho,[1,a] Sang Wook Park,[1,a] Seungmin Baek,[1,a] Donghwan Yun,[a] Gwang Yong Shin,[a] Hyeonsu Son,[b,c] Seyeong Song,[d] Hye Won Cho,[e] Hyeseon Shin,[a] Tae Kyung Lee *[b,c] and Gi-Hwan Kim *[a,d,e]

[a]Department of Materials Engineering and Convergence Technology, Gyeongsang National University (GNU), 501 Jinju-daero, Jinju 52828, Republic of Korea

[b]Department of Organic and Nano Engineering, Hanyang University, 222 Wangsimni-ro, Seongdong-gu, Seoul 04763, Republic of Korea

[c]Human-Tech Convergence Program, Hanyang University, 222 Wangsimni-ro, Seongdong-gu, Seoul 04763, Republic of Korea

[d]Research Institute of Molecular Alchemy, Gyeongsang National University (GNU), 501 Jinju-daero, Jinju 52828, Republic of Korea

[e]College of Space and Aeronautics, Gyeongsang National University (GNU), 501 Jinju-daero, Jinju 52828, Republic of Korea

[1]Y. Cho, S. W. Park, and S. Baek contributed equally to this work.

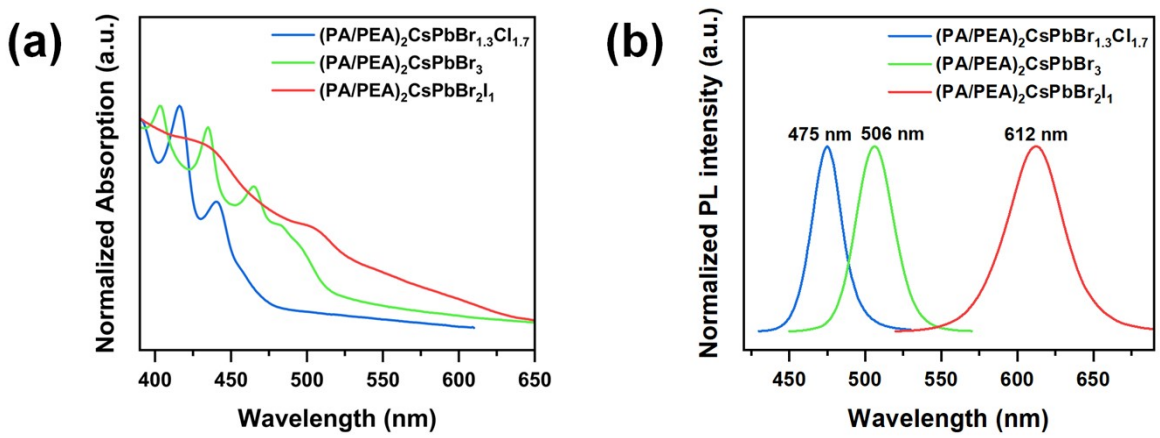

Fig. S1 Optical characteristics of pristine quasi-2D perovskite. (a) UV-visible absorption spectra. (b) Photoluminescence spectra.

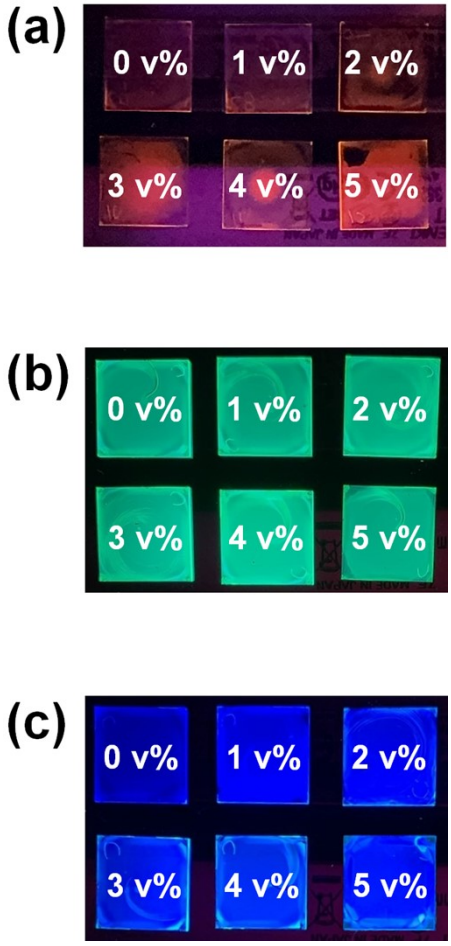

Fig. S2 Photoluminescence images of perovskite films prepared with iron additive concentrations (0–5 v%) under UV lamp illumination. (a) Red films. (b) Green films. (c) Blue films.

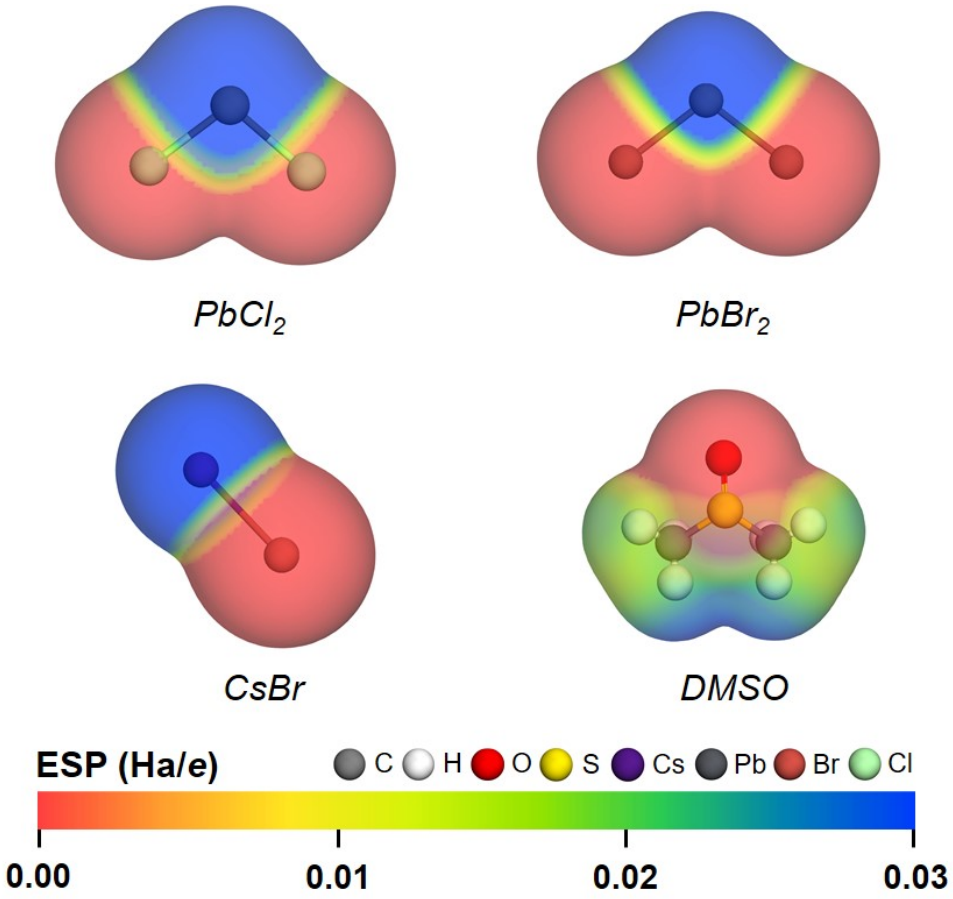

Fig. S3 Electrostatic potential (ESP) isosurfaces of $PbCl_2$, $PbBr_2$, CsBr, and DMSO molecules. The isosurface value is 0.03 e/Å^3.

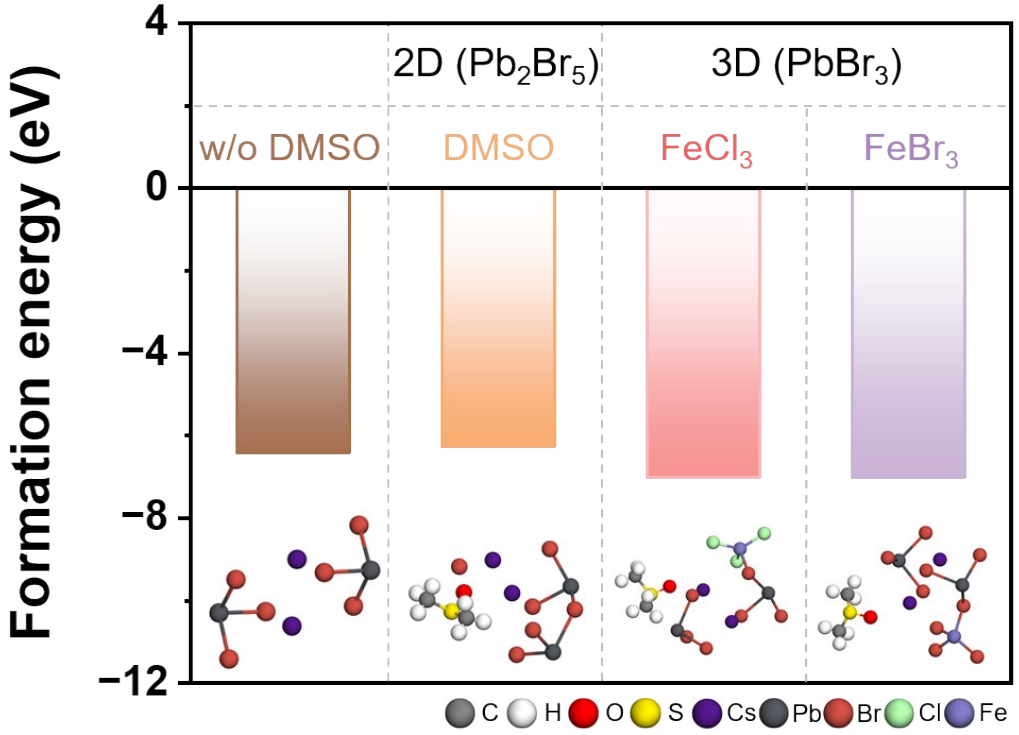

Fig. S4 Optimized structures and formation energies of 2D (Pb_2Br_5-based) and 3D ($PbBr_3$-based) structures in the green perovskite precursor system under different conditions (*i.e.*, w/o DMSO, DMSO, $FeCl_3$, and $FeBr_3$).

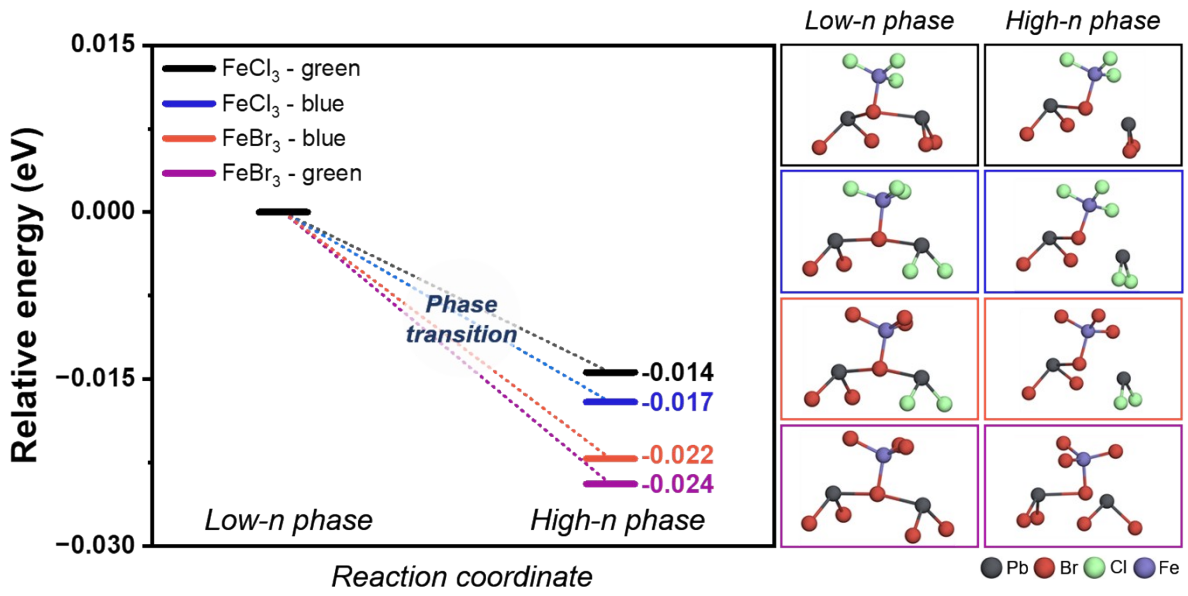

Fig. S5 Relative energy profiles of phase transition from low-n phases to high-n phases induced by iron additives in green and blue precursor systems.

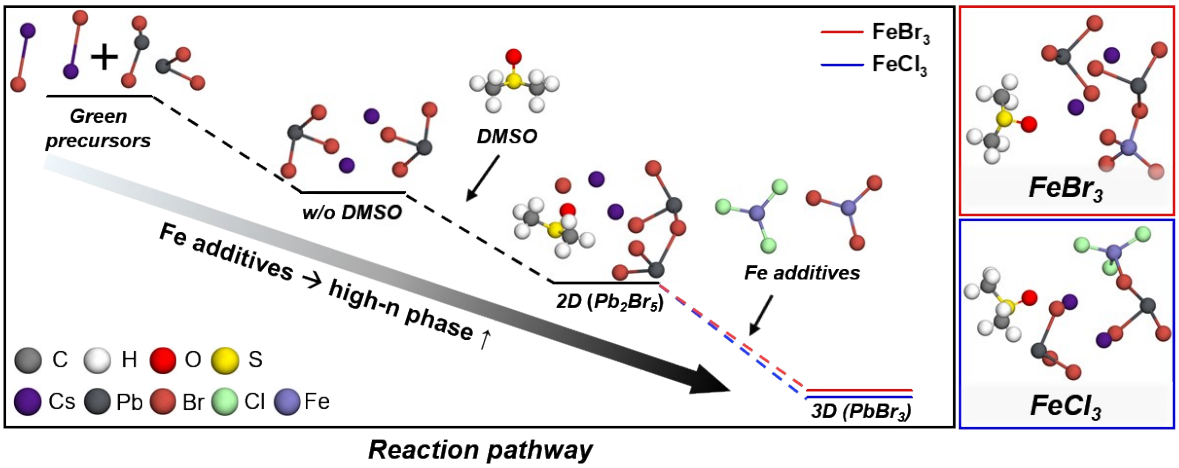

Fig. S6 Schematic reaction pathway of the phase transition from Pb_2Br_5 to $PbBr_3$ in the green precursor system.

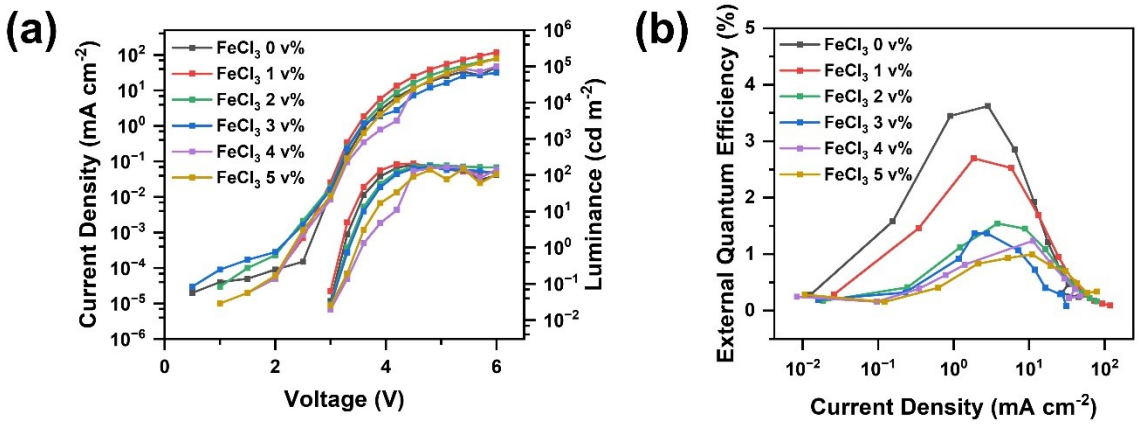

Fig. S7 Characteristics of blue PeLEDs with initial concentration of $FeCl_3$ additives. (a) *J-V-L* curves, (b) EQE-*J* curves.

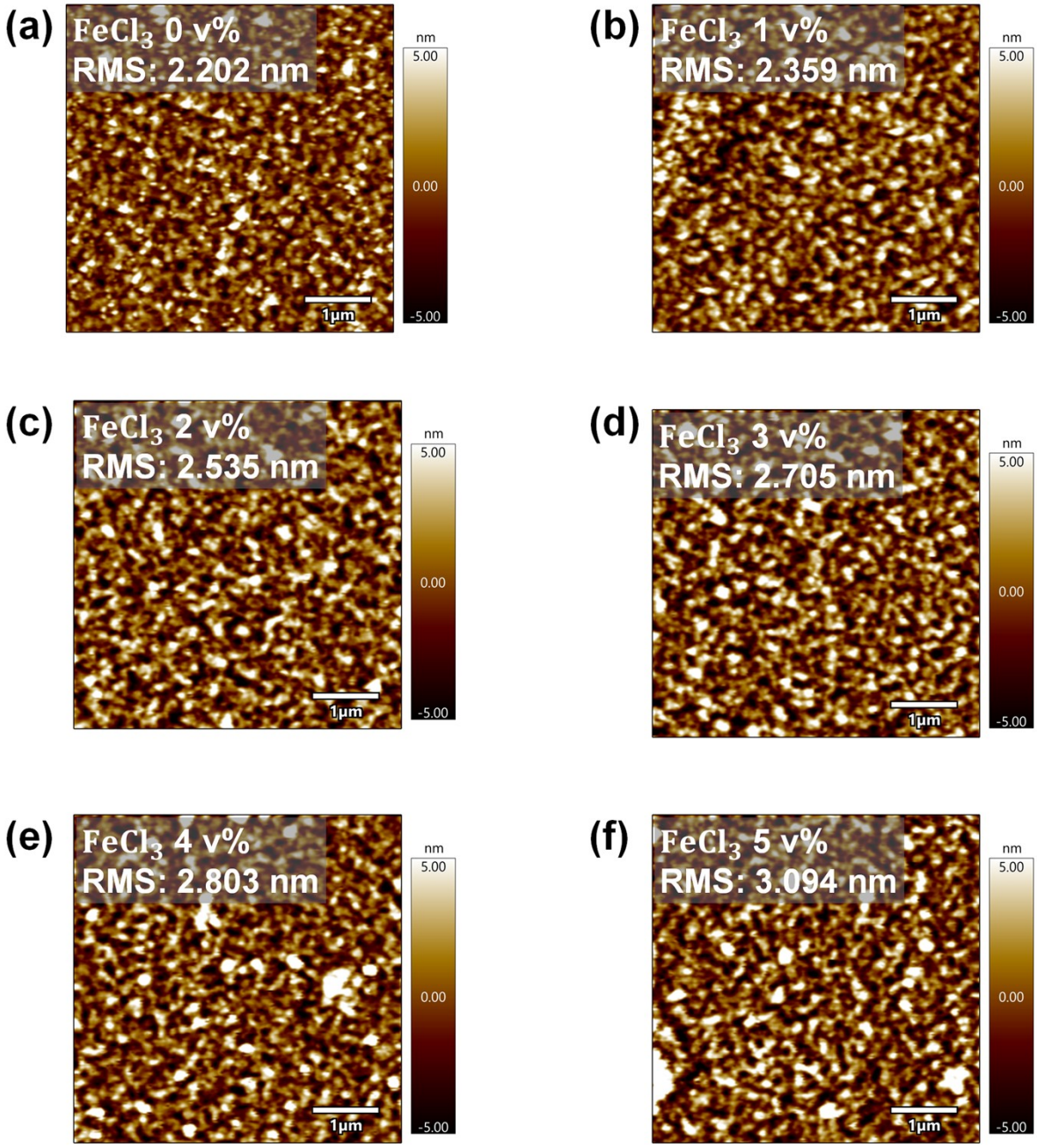

Fig. S8 AFM topography images of quasi-2D perovskite films with initial concentration of $FeCl_3$ additives: (a) 0 v%, (b) 1 v%, (c) 2 v%, (d) 3 v%, (e) 4 v%, and (f) 5 v%.

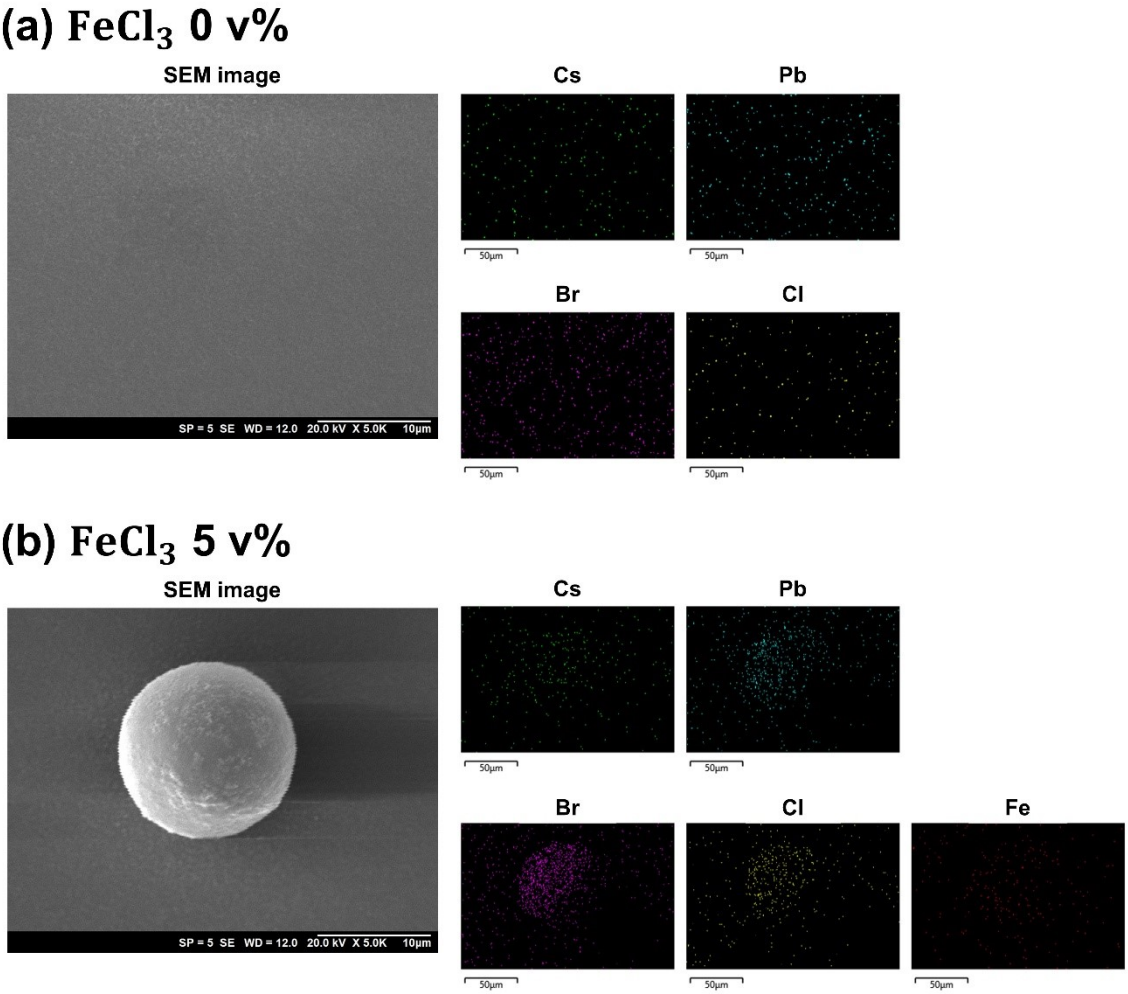

Fig. S9 SEM images and corresponding EDS elemental mapping of quasi-2D perovskite films with initial concentration of $FeCl_3$ additives: (a) 0 v% and (b) 5 v%.

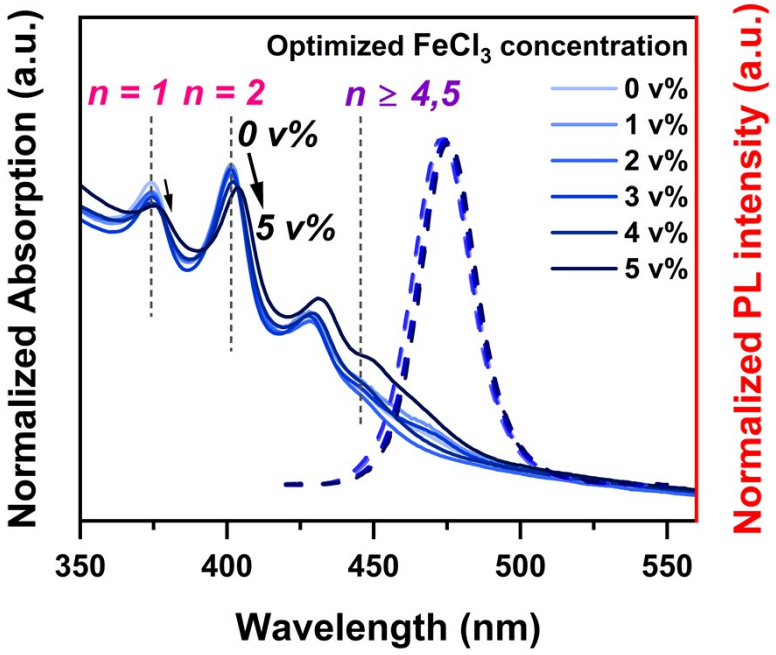

Fig. S10 UV-visible absorption and photoluminescence spectra of blue emission perovskite with optimized concentration of $FeCl_3$ additives.

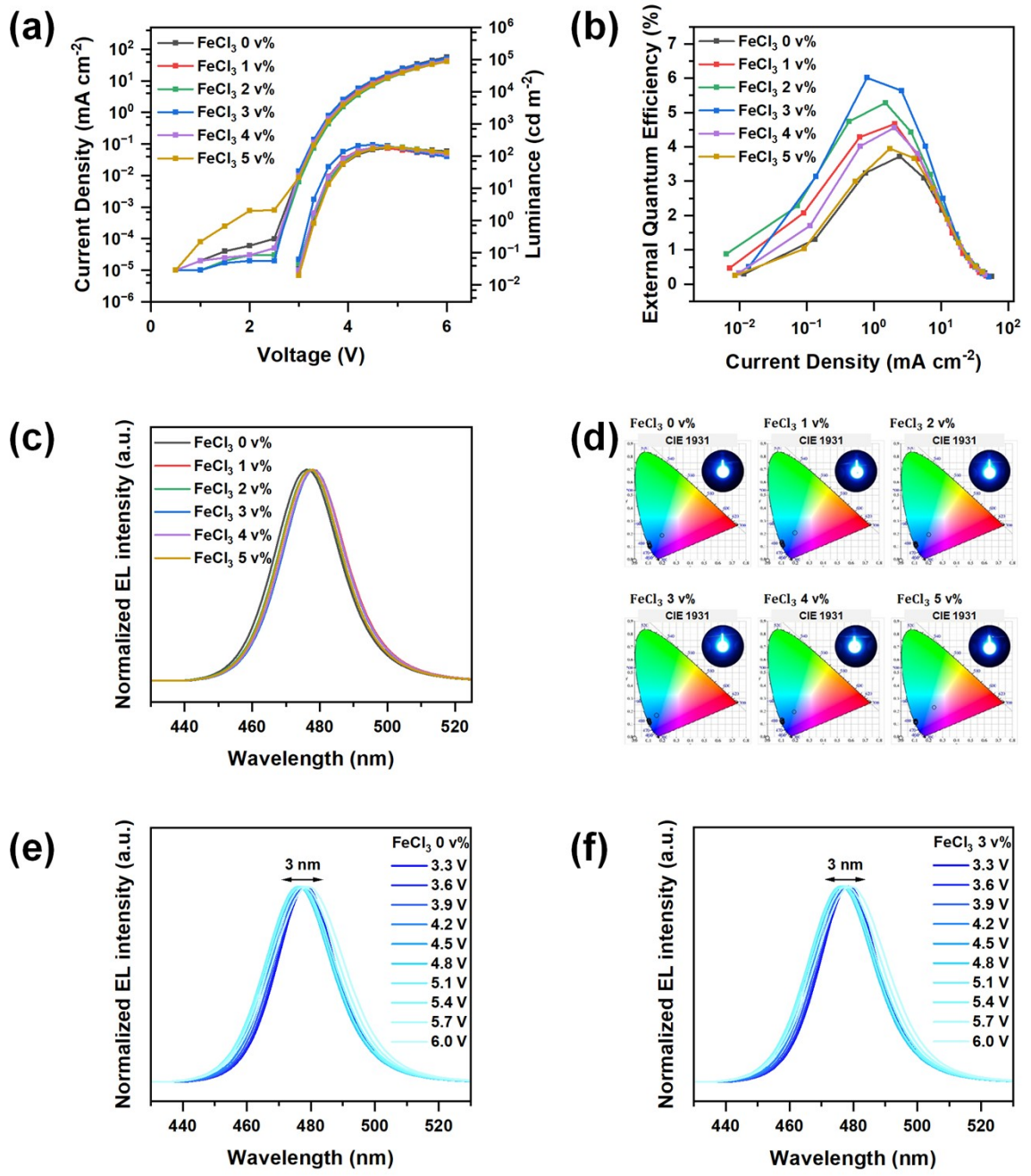

Fig. S11 Characteristics of blue PeLEDs with optimized concentration of $FeCl_3$ additives. (a) *J-V-L* curves, (b) EQE-*J* curves, (c) electroluminescence spectra, and (d) CIE coordinates of the blue PeLEDs (inset shows a photograph of an operating PeLEDs). Electroluminescence spectra according to the applied voltages of (e) $FeCl_3$ 0 v% and (f) $FeCl_3$ 3 v%.

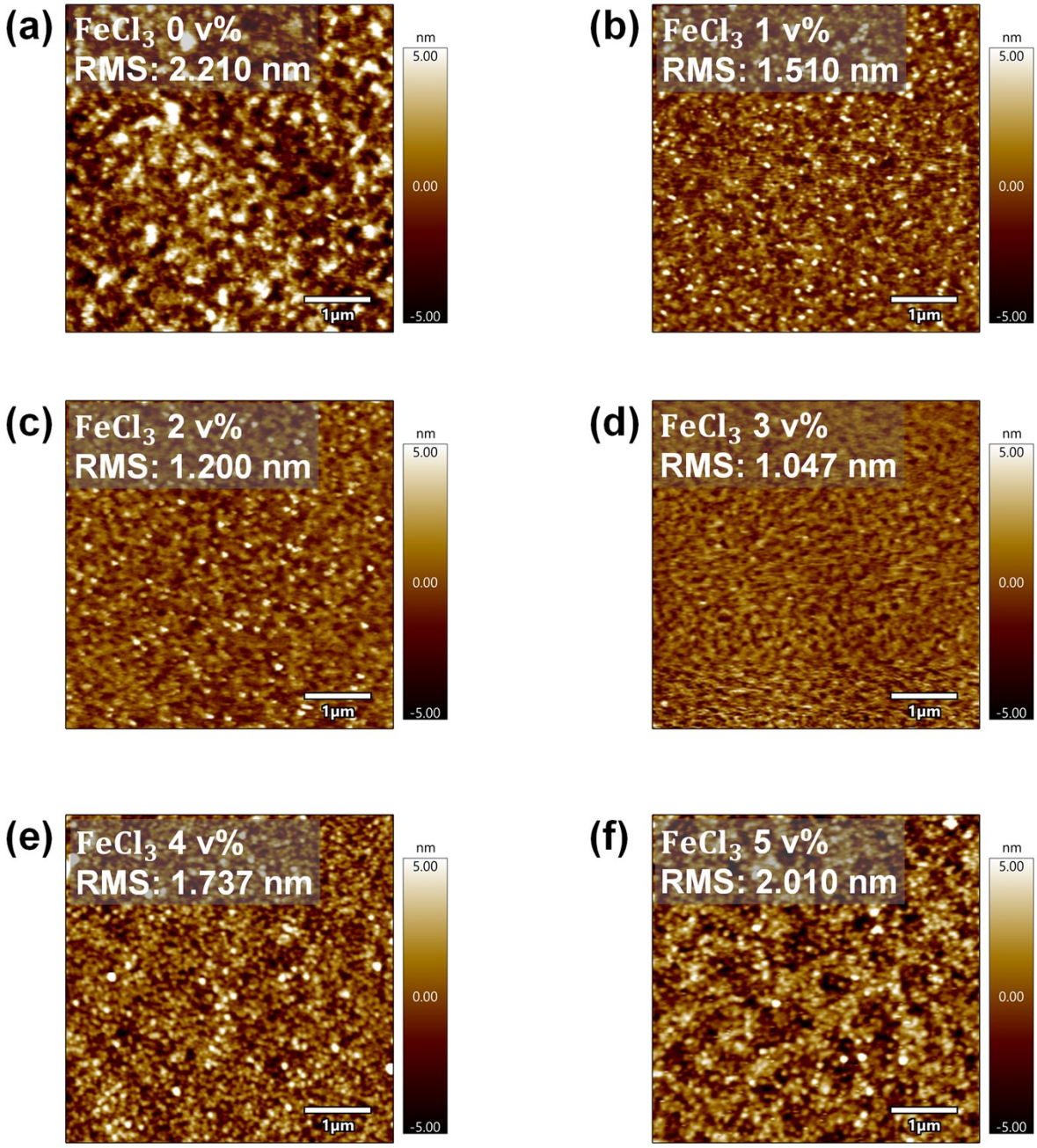

Fig. S12 AFM topography images of quasi-2D perovskite films with optimized concentration of $FeCl_3$ additives: (a) 0 v%, (b) 1 v%, (c) 2 v%, (d) 3 v%, (e) 4 v%, and (f) 5 v%.

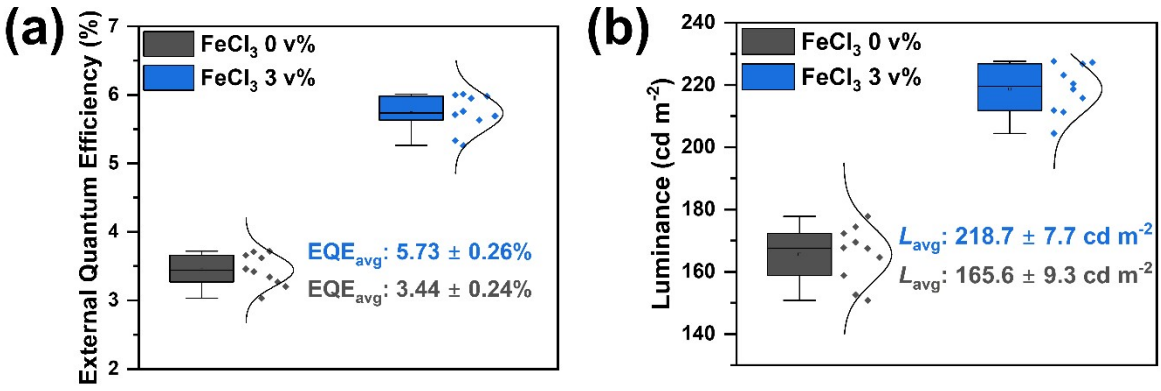

Fig. S13 Average values and standard deviations (a) EQE and (b) luminance for 10 devices.

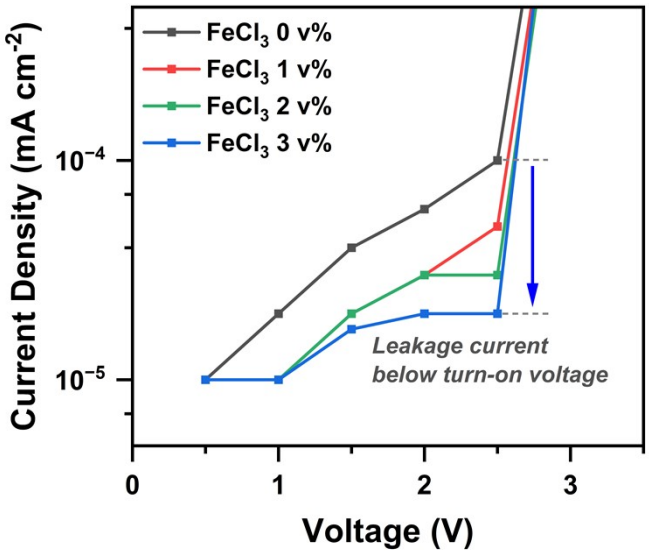

Fig. S14 Enlarged J–V curves below the turn-on voltage showing reduced leakage current with increasing $FeCl_3$ concentration.

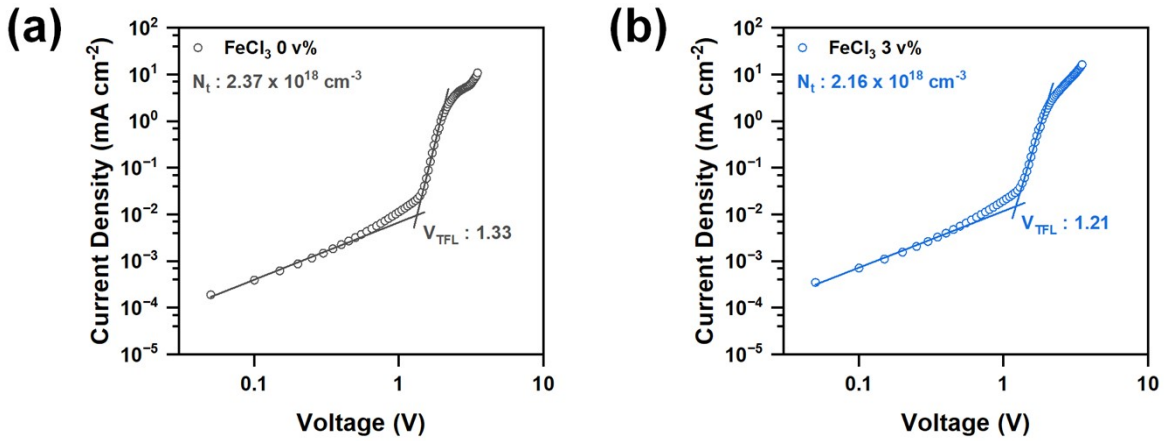

Fig. S15 The space-charge-limited current (SCLC) of quasi-2D perovskite hole-only devices of (a) $FeCl_3$ 0 v% and (b) $FeCl_3$ 3 v%.

Table S1. Photoluminescence wavelength and FWHM of quasi-2D perovskite with additives.

Additive volume ratios	Red + $FeBr_3$		Green + $FeBr_3$		Blue + $FeCl_3$	
	Wavelength (nm)	FWHM (nm)	Wavelength (nm)	FWHM (nm)	Wavelength (nm)	FWHM (nm)
0 v%	612	43.7	506	30.8	475	28.0
1 v%	612	42.8	506	26.7	476	27.3
2 v%	613	41.8	508	26.0	479	26.6
3 v%	615	41.3	509	23.8	480	26.2
4 v%	617	40.2	509	23.3	480	25.9
5 v%	621	39.6	510	22.5	481	25.8

Table S2. Device characteristics of blue PeLEDs with initial concentration of $FeCl_3$ additives.

Additive concentrations	Turn on voltage (V)	Luminance max (cd/m^2) @ voltage (V)	EQE max (%) @ voltage (V)	EL peak (nm)
0 v%	3.3	192.1 @ 4.5	3.62 @ 3.9	476
1 v%	3.3	205.0 @ 4.5	2.70 @ 3.6	479
2 v%	3.3	188.5 @ 4.8	1.54 @ 3.9	479
3 v%	3.3	170.5 @ 4.8	1.37 @ 3.9	479
4 v%	3.3	164.1 @ 5.1	1.24 @ 4.5	480
5 v%	3.3	149.0 @ 5.4	1.00 @ 4.5	480

Table S3. Photoluminescence wavelength and FWHM of quasi-2D perovskite with optimized concentration of $FeCl_3$ additives.

Additive volume ratios	Blue + $FeCl_3$	
	Wavelength (nm)	FWHM (nm)
0 v%	474	23.8
1 v%	474	23.8
2 v%	474	23.6
3 v%	475	22.9
4 v%	476	22.6
5 v%	476	22.2

Table S4. Device characteristics of blue PeLEDs with optimized concentration of $FeCl_3$ additives.

Additive concentrations	Turn on voltage (V)	Luminance max (cd/m^2) @ voltage (V)	EQE max (%) @ voltage (V)	EL peak (nm)
0 v%	3.3	177.8 @ 4.8	3.72 @ 3.9	476
1 v%	3.3	182.1 @ 4.5	4.67 @ 3.9	477
2 v%	3.3	194.4 @ 4.8	5.28 @ 3.9	477
3 v%	3.3	227.6 @ 4.5	6.01 @ 3.6	478
4 v%	3.3	192.5 @ 4.8	4.56 @ 3.9	478
5 v%	3.3	189.3 @ 4.8	3.95 @ 3.9	478

Table S5. Electroluminescence wavelength and FWHM of quasi-2D perovskite LEDs with additives.

Additive volume ratios	Blue + $FeCl_3$	
	EL Wavelength (nm)	EL FWHM (nm)
0 v%	476	23.2
1 v%	477	22.8
2 v%	477	22.5
3 v%	478	22.2
4 v%	478	22.2
5 v%	478	21.8

Table S6. Triexponential fitting parameters for PL lifetimes of blue-emitting quasi-2D perovskite films with $FeCl_3$ additives.

Additive concentrations	τ_1 (ns)	f_1 (%)	τ_2 (ns)	f_2 (%)	τ_3 (ns)	f_3 (%)	τ_{avg} (ns)	χ^2
0 v%	0.79	46.53	7.93	33.16	60.81	20.31	1.57	1.35
3 v%	2.26	40.25	13.22	42.63	84.97	17.11	4.71	1.44